Neuropsychiatric Disease and Treatment

Dovepress
Taylor & Francis Group

Open Access Full Text Article

ORIGINAL RESEARCH

Discriminative Plasma Lipidomic Signatures of Dementia with Lewy Bodies and Alzheimer's Disease: A Targeted Mass Spectrometry and Machine Learning Approach

Lulu Wen[1,*], Yifei Zhang[2,*], Yuting Nie[1], Huixin Shen[1], Qi Qin[1], Miao Qu[1]

[1]Neurology Department, Xuanwu Hospital of Capital Medical University, Beijing, People's Republic of China; [2]College of Arts and Science, New York University, New York, NY, 10003, USA

*These authors contributed equally to this work

Correspondence: Miao Qu; Qi Qin, Email qumiao@xwhosp.org; qinqi@xwhosp.org

Background: Dementia with Lewy bodies (DLB) exhibits a more aggressive progression and poorer prognosis than Alzheimer's disease (AD), yet clinical differentiation remains challenging. Dysregulated lipid metabolism, implicated in α-synuclein aggregation and neuroinflammation, may offer specific biomarkers for distinguishing DLB and AD.

Methods: This cross-sectional study implemented targeted lipidomic profiling to comprehensively characterize plasma lipidomes in a cohort comprising 50 DLB patients and 56 AD patients. Five machine learning algorithms - least absolute shrinkage and selection operator (LASSO) regression, support vector machine (SVM), random forest (RF), recursive feature elimination (RFE), and stepwise regression - were systematically applied for biomarker discovery.

Results: Significant alterations were observed in 7 lipid classes and 65 specific lipid species in DLB compared to AD. DLB plasma exhibited marked elevations in sphingolipids (total Cer, Hex1Cer, SM), lysophospholipids (LPC, LPE), phosphatidic acid (PA), alongside significant reductions in 45 triacylglycerol (TG) species compared to AD. Five machine learning algorithms consistently identified PA(16:0_16:0) and PA(16:0_20:4) as core discriminators between DLB and AD. The LASSO regression model demonstrated superior generalizability in the test set (AUC=0.916), selecting a 11-lipid panel dominated by PA species, alongside PC (18:0_20:4), ChE(22:4), Hex2Cer(d18:1_22:0), and PE species.

Conclusion: This first comprehensive targeted lipidomics study reveals distinct plasma lipid signatures differentiating DLB from AD, characterized by upregulated sphingolipids, lysophospholipids, and PA, and downregulated TG. Machine learning identified a 11-lipid biomarker panel, highlighting profound disturbances in glycerophospholipid metabolism. These findings provide novel molecular insights into DLB pathogenesis and a promising diagnostic tool for diagnosis.

Keywords: dementia with Lewy bodies, Alzheimer's disease, lipidomic signatures, machine learning, biomarker

Introduction

Alzheimer's disease (AD) is the leading cause of dementia, which is rapidly emerging as one of the most costly, deadly, and burdensome diseases of the 21st century. The latest data indicate that by 2050, the prevalence of dementia primarily caused by AD will double in Europe and triple worldwide.[1] In the United States, the prevalence of AD increases markedly with advancing age: 5% among those aged 65–74 years, 13.1% among those aged 75–84 years, and 33.3% among individuals aged 85 years and older.[2] Dementia with Lewy bodies (DLB), the second most common cause of neurodegenerative dementia after Alzheimer's disease (AD), accounts for approximately 4.2% of dementia diagnoses in community-based populations.[3] Epidemiological research indicates that the median survival time of DLB patients is merely 3–4 years, which is substantially shorter than the 5–10 years of AD patients,[4] suggesting a more aggressive

https://doi.org/10.2147/NDT.S561999
Received: 22 August 2025
Accepted: 27 February 2026
Published: 10 March 2026

clinical course and substantially poorer prognosis. The core clinical triad of DLB, fluctuating cognitive impairment, spontaneous parkinsonian syndrome, complex visual hallucinations, and rapid eye movement sleep behavior disorder, significantly impair quality of life, increase fall risk, and contribute to a hospitalization rate 1.9 times higher than that of AD patients.[5] Collectively, these factors impose a substantial socioeconomic and caregiver burden on DLB patients and families.

It is noteworthy that although the 2017 diagnostic criteria of the International Dementia with Lewy Bodies Consortium have further enhanced the diagnostic accuracy of DLB, a relatively high clinical misdiagnosis rate still persists.[6] Firstly, the clinical symptoms of DLB exhibit significant overlap with those of diseases such as AD. The fluctuations in cognitive and behavioral symptoms of DLB exacerbate the difficulty in differentiating it from AD.[7] Pathologically, DLB is characterized by Lewy bodies formed through α-synuclein deposition, whereas AD manifests with β-amyloid(Aβ) plaques and tau neurofibrillary tangles. However, clinical differentiation remains challenging due to biomarker overlap, as DLB patients frequently exhibit concurrent AD pathology (Aβ + Tau).[8] Neuropathological overlap also exists, with most DLB cases exhibiting concurrent AD pathology, blurring diagnostic boundaries.[9] In addition, dopamine transporter (DAT) single-photon emission computed tomography (SPECT) imaging and myocardial iodine-123 metaiodobenzylguanidine (MIBG) scintigraphy can be utilized to support the diagnosis of DLB. However, these methods are costly and have limited availability.[10] The detection of cerebrospinal fluid α-synuclein remains in the research phase, and the invasive nature of the procedure restricts its clinical application. Consequently, the search for blood-based metabolic markers holds significant clinical translational value. However, no blood-based diagnostic kit has been approved for clinically differentiating DLB from AD, highlighting the urgent need for developing novel biomarkers and methods to address this unmet clinical need.[11]

Lipids constitute over 50% of the brainstem's dry weight and are critical in maintaining membrane architecture, synaptic function, and energy metabolism.[12] In recent years, studies have shown that lipid metabolism dysregulation is closely associated with the abnormal aggregation of α-synuclein.[13] As a lipid-binding protein, α-synuclein undergoes conformational changes regulated by membrane lipid composition. Research has demonstrated that certain lipids, such as sphingomyelin and cholesterol, can facilitate the oligomerization of α-synuclein, leading to the formation of toxic fibrils.[14,15] Animal experiments have confirmed that deficiencies in lipid metabolism-related enzymes, such as glucocerebrosidase (GBA1), can cause lysosomal dysfunction, accelerate the aggregation of α-synuclein, and trigger neurodegeneration.[16,17] Our previous non-targeted metabolomics identified lipid disturbances in DLB involving phosphatidylcholine and sphingomyelin.[18] However, the semi-quantitative nature and relatively low throughput of non-targeted methods have limited their clinical translation.[19] Targeted lipidomics utilizing multiple reaction monitoring (MRM) achieves picomolar-level quantification, particularly critical for analyzing low-abundance sphingolipids.[20,21] The present study advances beyond this prior work by employing targeted LC-MS/MS with multiple reaction monitoring, achieving picomolar-level quantification of diverse lipid classes including glycerophospholipids and sphingolipids. This approach enables systematic mapping of DLB-specific lipid networks with higher precision and reproducibility.

Despite growing evidence of lipid dysregulation in both AD and DLB, comparative targeted lipidomic studies using quantitative, high-sensitivity platforms remain lacking. Most prior work has focused on single diseases or relied on non-targeted approaches with limited accuracy and lipid coverage. Moreover, no blood-based biomarker panel has been established to reliably distinguish DLB from AD using targeted lipidomics. This study aims to address this gap by quantitatively profiling plasma lipids in AD and DLB patients using targeted mass spectrometry, integrated with machine learning to identify differential diagnostic biomarkers.

Materials and Methods

Inclusion of Participants

This cross-sectional study was conducted at Xuanwu Hospital, Capital Medical University, and Guangnei Community Health Service Center between January 2021 and June 2022. The study protocol received approval from the Ethics Committee of Xuanwu Hospital (No.[2020]097) and was conducted in accordance with the Declaration of Helsinki. A total of 106 participants (50 DLB patients, 56 AD patients) were consecutively enrolled following written informed

consent. AD diagnoses were established according to the National Institute on Aging–Alzheimer's Association (NIA-AA) criteria incorporating the ATN biomarker framework (amyloid-β [A], tau [T], neurodegeneration [N]).[22] All patients with DLB met the criteria for probable DLB followed the 2017 international consensus criteria.[23] Patients with possible DLB were excluded from the study. Diagnostic confirmation required unanimous agreement by three neurologists specializing in neurodegenerative disorders. Exclusion criteria included a history of mental illness such as schizophrenia, bipolar disorder and major depressive disorder with psychotic features, excessive alcohol consumption, a history of autoimmune diseases, reversible cognitive impairment including B12 deficiency and hypothyroidism, organic brain injury, a history of brain surgery, long-term use of steroid hormones, and malignant tumors that might affect the results.

General Information and Scale Assessment

Baseline demographic characteristics and comorbidities were systematically documented to support for subsequent analysis. Cognitive function was assessed using validated instruments: the Clinical Dementia Rating (CDR), and Montreal Cognitive Assessment (MoCA).[24,25] Certified neuropsychologists administered all tests following standardized protocols to ensure inter-rater reliability.

Plasma Sample Preparation

Venous blood (6 mL) was collected from fasting participants using EDTA-K2 anticoagulant tubes. Samples were immediately centrifuged (3000 g, 10 min, 4°C). Plasma aliquots (500 μL) were flash-frozen in liquid nitrogen and stored at −80°C until detection.

Lipid Extraction and Processing, Chromatographic Separation Parameters and Mass Spectrometry Detection Parameters

The lipid extraction, sample processing, chromatographic separation, and mass spectrometry detection were carried out by Shanghai Applied Protein Technology Co., Ltd. (Shanghai, China). Lipids were extracted according to methyl tert-butyl ether (MTBE) method. Frozen plasma was thawed at 4°C, and a quantitative sample was mixed with 200 μL of methanol and vortexed. Then, 20 μL of isotope-labeled internal standard solution was added, followed by 800 μL of MTBE. The mixture was thoroughly shaken and mixed. After low-temperature ultrasonic treatment (20 min) and room-temperature standing (30 min), 200 μL of ultrapure water was added, vortexed vigorously, and centrifuged at 4°C at 14,000 rpm for 15 min to separate the layers. The organic phase was dried under nitrogen, and 200 μL of 90% isopropanol/acetone mixture was added for reconstitution. After centrifugation, the supernatant was taken for injection.

Analyses were performed on an UHPLC-MS/MS system (Nexera LC-30A, Shimadzu). The temperature of the reversed-phase C18 column (Phenomenex, Kinetex C18, 2.1×100 mm, 2.6 μm) was set at 45°C. For RPLC separation, the column temperature was set at 45°C. Mobile phase A: 70% acetonitrile+30%H2O+5mM ammonium acetate, mobile phase B: IPA solution. A gradient (20% B at 0 min, 60% B at 5 min, 100% B at 13 min, 20% B at 13.1–17 min) was then initiated at a flow rate of 0.35 mL/min. The sample was placed at 10 °C during the whole analysis process. For HILIC separation, the column temperature was set at 40 °C. Mobile phase A: 2mM ammonium acetate +50% methanol+50% acetonitrile, mobile phase B: 2mM ammonium acetate +50% acetonitrile +50% water. A gradient (3% B at 0–3 min, from 3% to 100% B at 3–13 min, 100% B at 13–17 min, 3% B at 17.1 −22 min) was then initiated at a flow rate of 400 μL/min.

6500+ QTRAP (AB SCIEX) was performed in positive and negative switch mode. The ESI positive source conditions were as follows: Source temperature: 400°C; Ion Source Gas1 (GS1): 50 Ion Source Gas2 (GS2): 55; Curtain Gas (CUR): 35; IonSpray Voltage (IS): +5500 V; The ESI negative source conditions were as follows: Source temperature: 400°C; Ion Source Gas1 (GS1): 50; Ion Source Gas2 (GS2): 55; Curtain gas (CUR): 35; IonSpray Voltage (IS): −4500 V. MRM method was used for mass spectrometry quantitative data acquisition.

Statistical Analysis

All continuous variables underwent normality assessment via Shapiro–Wilk tests, with parametric distributions analyzed by Student's *t*-test and non-parametric distributions by Wilcoxon tests. Categorical variables were evaluated using Pearson's χ^2-tests. Statistical analyses were conducted in IBM SPSS Statistics (v27.0; Armonk, NY), with significance thresholds set at $P < 0.05$. QC workflow of targeted lipidomics: Pooled QC samples were injected every 10 study samples to monitor instrument stability; lipid features with CV > 30% in QCs were excluded to ensure reproducibility; and QC-based robust LOESS normalization was applied to correct signal drift and batch effects. PCA of QC samples showed no significant batch clustering after correction, confirming effective removal of systematic error. For targeted lipidomics data preprocessing, metabolites with > 30% missing values across all samples were excluded from further analysis. For the remaining metabolites, missing values were imputed using half of the minimum detected value for each metabolite, an approach appropriate for targeted lipidomics datasets where missing values are predominantly attributable to concentrations below the limit of detection (Missing Not At Random, MNAR).[26] To adjust for significant between-group differences in age and sex, each lipid feature was regressed on these variables, and the residuals were used as confounder-adjusted values for all subsequent analyses—a widely adopted approach in metabolomics that removes demographic confounding while preserving biological signals.[27,28] Targeted lipidomics data were processed using Simca-P (v16.0.2, Sartorius Stedim Biotech). First, the data were normalized by Pareto scaling, and Hotelling T^2 test was used to identify outliers. Then, model establishment and calculation were carried out. Metabolites with VIP ≥ 1 and adj $P < 0.05$ were considered statistically significant. Lastly, the differential metabolite dataset was randomly split into training (70%) and test (30%) sets using stratified sampling.Five machine learning algorithms were selected based on their complementary strengths: LASSO (L1 regularization, λtuned by 5-fold CV with min binomial deviance), random forest (mtry optimized by 5-fold CV, ntree=500), linear SVM (cost C optimized by grid search + 5-fold CV), RFE (random forest base learner, optimal feature subset determined by 5-fold CV maximizing AUC), and stepwise regression (bidirectional AIC-based selection)—all feature selection and hyperparameter tuning were performed exclusively within the training set, with the test set held out for final evaluation.

Results

Baseline Characteristics of DLB and AD Patients

The comparison of baseline characteristics between the DLB group (n=50) and AD group (n=56) is presented in Table 1. Patients in the DLB group were significantly older than those in the AD group (71.36 ± 6.85 years vs. 63.42 ± 9.70 years,

Table 1 Baseline Characteristics of DLB and AD Patients

Variables	DLB (n=50)	AD (n=56)	P
Age (years)	71.36± 6.85	63.42± 9.70	<0.001
Gender, males/females	30/20	22/34	0.033
Education [years, M (Q1, Q3)]	12 (6, 15)	10 (9, 13)	0.563
BMI (kg/m^2)	23.44 (21.85, 26.53)	23.44 (21.92, 25.42)	0.371
Hypertension,n (%)	25 (50.0%)	18 (32.7%)	0.072
Diabetes,n (%)	11 (21.6%)	6 (10.7%)	0.125
Stroke,n (%)	6(12%)	4(7.3%)	0.410
TC (mmol/L)	0.95 (0.7, 1.43)	1.27 (0.9, 2.02)	0.271
TG (mmol/L)	4.17 (3.6, 4.85)	4.77 (4.02, 5.51)	0.079
HDL (mmol/L)	1.21 (1.05, 1.58)	1.33 (1.2, 1.59)	0.263
LDL (mmol/L)	2.38 (2.08, 2.95)	2.8 (2.19, 3.45)	0.149
ApoA1 (g/L)	1.18 (1.05, 1.41)	1.32 (1.2, 1.46)	0.02
ApoB (g/L)	0.78 (0.69, 0.95)	0.88 (0.71, 1.06)	0.124
MoCA [scores, M (Q1, Q3)]	12.68±6.12	12.68±6.82	0.856
CDR [scores, M (Q1, Q3)]	1 (0.5, 2)	1 (1, 1.26)	0.194

Abbreviations: BMI, Body Mass Index; TC, Total Cholesterol; TG, Triglycerides; HDL, High-Density Lipoprotein; LDL, Low-Density Lipoprotein; ApoA1, Apolipoprotein A1; ApoB, Apolipoprotein B; MoCA, Montreal Cognitive Assessment; CDR, Clinical Dementia Rating.

p < 0.001) and had a higher proportion of males (p = 0.033). No statistically significant differences were observed between the two groups in terms of education duration, body mass index(BMI), history of hypertension, diabetes and history of stroke (all p > 0.05).Lipid profile analysis revealed that the DLB group had lower apolipoprotein A1 levels (1.18 [1.05, 1.41] g/L vs. 1.32 [1.20, 1.46] g/L, p = 0.02), while no significant intergroup differences were found in total cholesterol (TC), triglycerides (TG), high-density lipoprotein (HDL), low-density lipoprotein (LDL), or apolipoprotein B levels (all p > 0.05). Cognitive assessment demonstrated no significant differences in MoCA, or CDR scores between groups (all p > 0.05), suggesting comparable levels of cognitive impairment in both groups.

Differential Plasma Lipid Classes Between DLB and AD

To elucidate lipid metabolism differences between DLB and AD, we performed targeted lipidomics profiling in patient plasma. Given the differences in age and sex between DLB and AD patients, we referred to previous studies and analyzed differential metabolites using metabolomics data adjusted for age and sex.[18] A total of 7 lipid classes exhibiting replicable and statistically significant alterations were identified (Figure 1 and Supplementary Table 1). Firstly, sphingolipid substances were detected. The total ceramide (Cer) level in the plasma of DLB patients was significantly higher than that of AD (1966.78 ± 581.99 vs. 1729.93 ± 634.95, $P < 0.05$), and hexanoyl ceramide (Hex1Cer) (1090.98 ± 368.25 vs. 920.36 ± 269.39, P < 0.01) and sphingomyelin (SM) were significantly increased in the DLB group (11091.51 ± 1174.36 vs. 10463.44 ± 1178.21, P < 0.01). These results suggest that the disruption of sphingolipid metabolism may be involved in the pathogenesis of DLB. Secondly, relevant were conducted for glycerophospholipid substances. Lysophosphatidylcholine (LPC) (8157.56 ± 1769.43 vs. 6980.91 ± 1417.24, P < 0.001) and lysophosphatidylethanolamine (LPE) (830.93 ± 258.79 vs. 672.92 ± 229.16, P < 0.01) significantly increased in the DLB group, suggesting that the phospholipid remodeling process may be affected. Additionally, phosphatidic acid (PA) increased most significantly in the DLB group (4687.88 ± 997.74 vs. 3581.58 ± 824.06, P < 0.001). Besides, the triglyceride (TG) level in DLB patients was significantly lower than that in the AD group (102877.82 ± 33,352.15 vs. 138107.90 ± 45,326.40, P < 0.001).Notably, total TG measured by conventional clinical assay showed a trend toward lower levels in DLB but did not reach statistical significance (P = 0.079, Table 1). This discrepancy reflects the higher analytical precision of LC-MS/MS, which quantifies each TG species individually, eliminates free glycerol interference, and applies equimolar response correction, thereby enabling more sensitive detection of true TG metabolic alterations in DLB.[29]

Distinct Alterations in Specific Lipid Molecular Species Differentiate DLB from AD

Our comprehensive lipidomic analysis employing multivariate statistical approaches revealed distinct molecular lipid signatures differentiating DLB from AD patients. The robustness of OPLS-DA model was confirmed through permutation testing (Figure 2A), demonstrating reliable predictive capability without overfitting. Both PCA (Figure 2B) and OPLS-DA (Figure 2C) analyses showed clear separation between DLB and AD groups, indicating potential differences in their plasma lipid profiles.

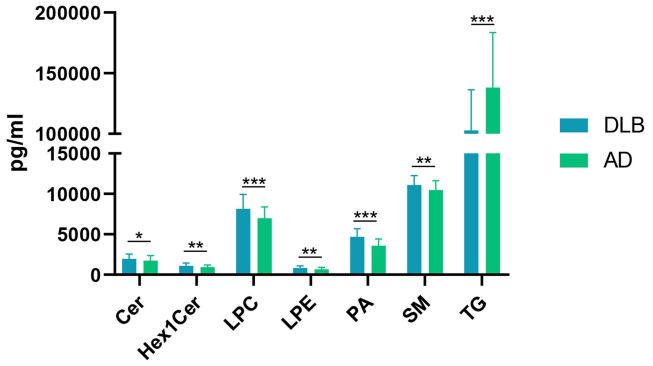

Figure 1 Differential Plasma Lipid Profiles Between DLB and AD.
Notes: *Represeents P<0.05, **Represeents P<0.05, ***Represeents P<0.05.
Abbreviations: Cer, ceramide; Hex1Cer, hexanoyl ceramide; LPC, lysophosphatidylcholine; LPE, lysophosphatidylethanolamine; PA, phosphatidic acid; TG, triglyceride.

https://doi.org/10.2147/NDT.S561999

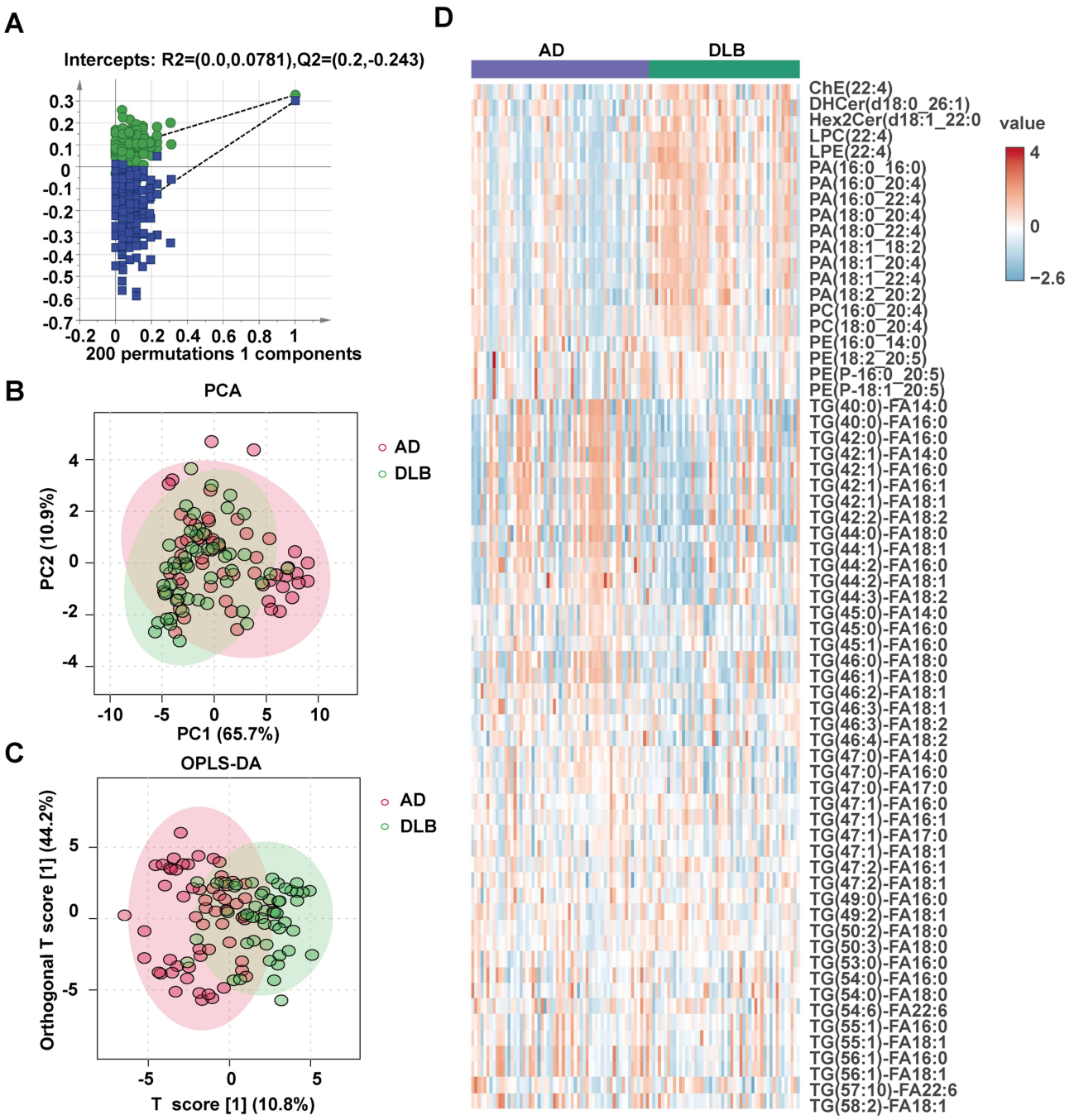

Figure 2 Distinct Alterations in Specific Lipid Molecular Species Differentiate DLB from AD.
Notes: (**A**) Permutation test plot. (**B**) PCA score plot showing distinct separation between DLB and AD groups. (**C**) OPLS-DA score plot revealing significant intergroup differences between DLB and AD groups. (**D**) Heatmap of differential metabolites (Red: upregulated in DLB; Blue: downregulated in DLB).

Our lipidomic analysis identified 65 significantly altered lipid molecular species (Supplementary Table 2), revealing distinct metabolic perturbations in DLB compared to AD. Notably, we observed marked elevations in specific sphingolipids, such as DHCer(d18:0_26:1) and Hex2Cer, and lysophospholipids, such as LPC(22:4) and LPE(22:4), along with significant increases in 9 phosphatidic acid (PA) species, 2 phosphatidylcholine (PC) species and 4 phosphatidylethanolamine (PE) species. Conversely, we detected a striking decrease in 45 triacylglycerol (TG) species alongside upregulation of cholesterol ester ChE(22:4) in DLB compared to AD (Figure 2D). These findings may also demonstrate profound disturbances across multiple lipid metabolic pathways in DLB, particularly affecting sphingolipid metabolism, phospholipid remodeling, and neutral lipid homeostasis.

https://doi.org/10.2147/NDT.S561999

Machine Learning for Screening of Differential Metabolic Markers Between DLB and AD

To identify plasma metabolomic signatures capable of distinguishing DLB from AD, we employed five distinct feature selection methods: LASSO regression, stepwise regression, Random Forest (RF), Recursive Feature Elimination (RFE), and linear Support Vector Machine (SVM). A notable convergence was observed among the features selected by these diverse algorithms (Figure 3A), underscoring the consistency and potential biological relevance of the identified markers. The number of selected features varied across methods according to their selection stringency (Figure 3B). RFE retained the highest number of features (n=15), followed by SVM (n=14), LASSO regression (n=11), and stepwise regression (n=7), with RF exhibiting the most conservative selection (n=5). The complete list of features selected by each individual machine learning approach is detailed in Supplementary Table 3. Critically, two phosphatidylcholine species, PA (16:0_16:0) and PA(16:0_20:4), were unanimously selected by all five methodologies (Figure 3C). This consistent identification strongly implicates these specific phospholipid molecules as playing a pivotal role in differentiating DLB from AD pathogenesis, suggesting they serve as core biomarkers for disease classification.

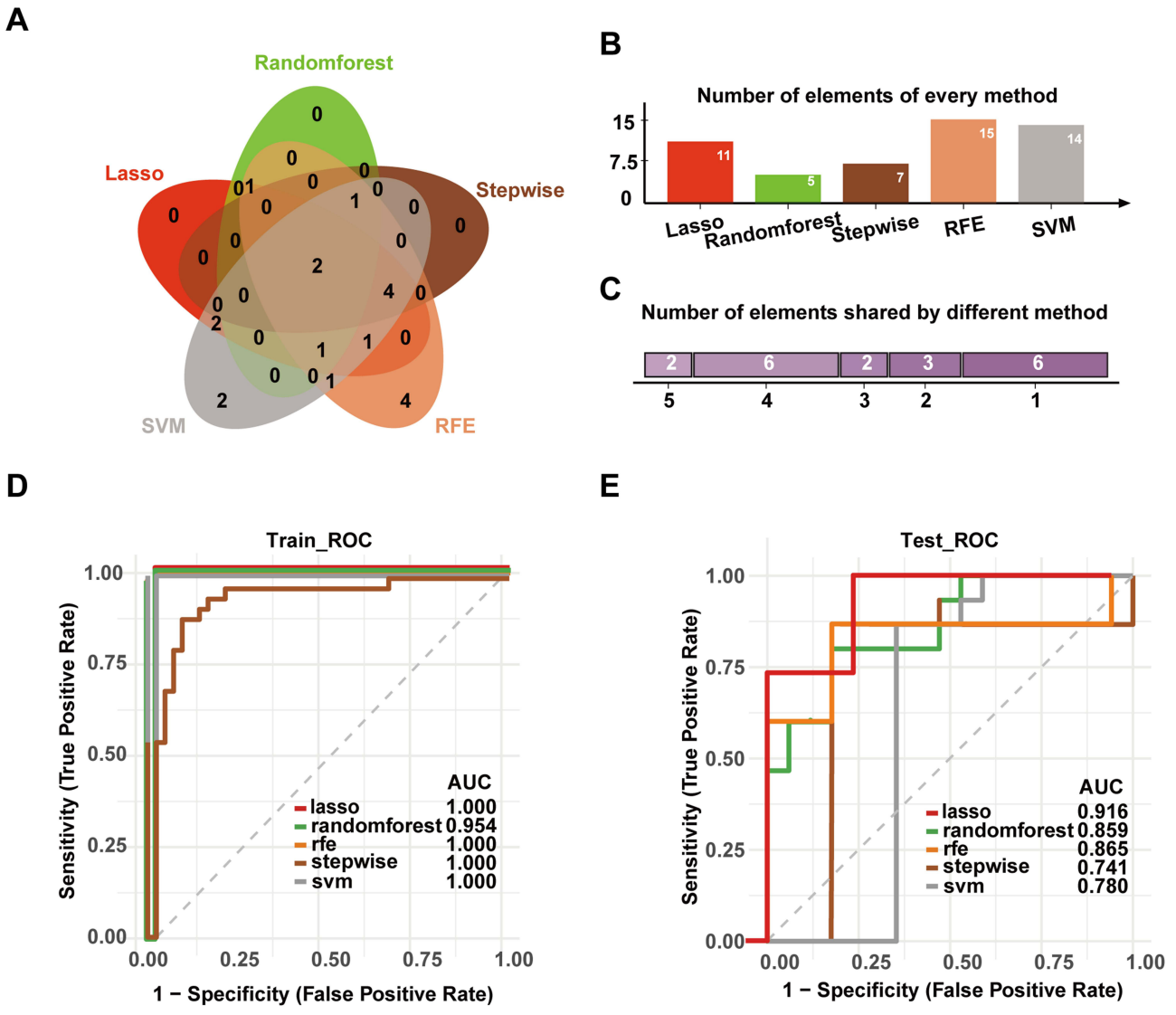

Figure 3 Machine learning for screening of differential metabolic markers between DLB and AD.
Notes: (**A**) Venn diagram showing the feature selection by various machine learning methods. (**B**) Bar chart presenting the number of features selected by each method. (**C**) Heatmap showing the selection of molecules in various methods. (**D** and **E**) Comparison of ROC curves of each model in the training set (**D**) and the test set (**E**).

https://doi.org/10.2147/NDT.S561999

Comprehensive evaluation of the five machine learning models revealed good performance in the training cohort, with all models achieving high AUC values (range: 0.954–1.000; Figure 3D). However, critical analysis of test set performance revealed significant differences in generalizability. Among the evaluated methods, LASSO regression demonstrated superior diagnostic efficacy in the test set, achieving the highest AUC (0.916). This performance surpassed that of stepwise regression (test AUC=0.741), linear SVM (test AUC=0.780), RF (test AUC=0.859), and RFE (test AUC=0.865), indicating its optimal balance between discriminative power and robustness against overfitting (Figure 3E).

The selection of LASSO regression was further justified by its inherent regularization mechanism that simultaneously performs feature selection and coefficient shrinkage to improve model generalizability. Using this optimized approach, we identified 11 highly discriminative lipid molecules, comprising six phosphatidic acids [PA(16:0_16:0), PA (16:0_20:4), PA(18:0_20:4), PA(18:1_20:4), PA(18:1_22:4), PA(18:2_20:2)], one phosphatidylcholine [PC(18:0_20:4)], one cholesteryl ester [ChE(22:4)], one hexosylceramide [Hex2Cer(d18:1_22:0)], and two phosphatidylethanolamines [PE (16:0_14:0), PE(P-18:1_20:5)]. This molecular signature, dominated by PA species implicated in synaptic vesicle trafficking and membrane dynamics, reflects significant perturbations in glycerophospholipid metabolism characteristic of DLB pathology.[30]

Discussion

This study provides the first comprehensive characterization of plasma lipidomic signatures differentiating DLB from AD using targeted lipidomics. Our analysis reveals possible lipid metabolic alterations related to the pathogenesis of DLB, with a total of 7 lipid classes showing changes, and 65 lipids showing significant differences compared to AD. These lipids are mainly concentrated in sphingolipid metabolism, and lysophospholipid/phosphatidylcholine classes, etc. We used various machine learning methods to screen variables and finally, the LASSO regression method determined a panel of optimal plasma differential metabolites that can effectively distinguish DLB from AD.

Sphingolipids constitute essential membrane constituents that orchestrate critical cellular processes, including cell membrane structure, signal transduction, cell recognition, and apoptosis, etc. The disorder of sphingolipid metabolism is closely related to the pathogenesis of various neuro-psychiatric diseases, such as AD, PD, brain injury, etc.[31–33] Our lipidomic profiling revealed significant elevations of ceramides (Cer), hexosylceramides (Hex1Cer), and sphingomyelins (SM) in DLB versus AD patients. Animal experiments have shown that Cer can promote the progression of AD by inducing microglial cell pyroptosis, and can also stabilize BACE-1 to promote Aβ generation and accumulation, while the level of Cer can significantly improve the cognitive impairment of rats.[34,35] Clinical studies have shown that high levels of ceramide in serum are associated with reduced hippocampal volume and increase the risk of AD.[36] A targeted plasma metabolomics study on AD also revealed a strong correlation between SM lipid classes and clinical dementia rating (CDR), suggesting that SM metabolic changes are closely related to the pathogenesis of AD.[37] Another plasma lipidomics study on AD revealed significant changes in HexCer metabolites in AD patients and was included in the diagnostic model of AD.[38] Prior untargeted metabolomics revealed elevated hexosylceramide (HexCer) levels in DLB compared to AD.[18] These collective findings implicate sphingolipid metabolism disorder as a possible neurodegeneration contributor, with DLB exhibiting greater metabolic perturbation magnitude than AD.

The possible pathogenesis of sphingolipid metabolism disorder in DLB may include the following factors: Firstly, Cer is an important component of cell membranes, which can mediate immune cell activation, inflammation, oxidative stress, metabolism, autophagy, and cell death, etc.[32,39] Elevated Cer may exacerbate inflammatory responses, induce mitochondrial dysfunction, promote α-synuclein aggregation, and aggravate the neurodegeneration of DLB.[40] Secondly, SM is also the main component of cell membranes, and its hydrolysis produces a large amount of ceramide, and the two are often positively correlated.[41] Elevated SM itself may also affect membrane fluidity, signal transduction, and apolipoprotein function.[42] Studies have found that SM-induced processing of neuronal cells induces the overexpression of ATP-binding cassette subfamily A5 (ABCA5) transporter (a group of proteins that transport lipids around the brain) and α-Syn, supporting the role of SM in inducing PD.[43] Furthermore, DLB and PD often have similar pathological bases, that is, the accumulation of α-Syn.[7] Therefore, SM may promote the occurrence of DLB by directly promoting the accumulation of α-Syn and indirectly producing Cer. Collectively, these findings demonstrate that sphingolipid dysregulation, particularly within Cer and SM, constitutes a distinct pathogenic signature differentiating DLB from AD. Mechanistically, this

dyshomeostasis may drive DLB progression through α-synuclein fibrillization potentiation and neuroinflammatory amplification.

In this study, LPC, LPE, and PA in DLB were significantly higher than those in AD. Previous studies have shown that serum LPE demonstrates diagnostic utility in differentiating AD patients from cognitively normal controls, with emerging predictive value for MCI-to-AD progression.[44] Align with our study, research on post-mortem brain tissue from AD patients revealed significantly elevated levels of LPE and PA, while LPC levels showed a significant positive correlation with Aβ deposition.[45,46] A preliminary small-sample study further indicated that plasma LPC may serve as a biomarker for distinguishing AD from DLB.[47] Collectively, these results underscore the important role of LPC, LPE and PA metabolic dysregulation in the pathogenesis of both DLB and AD, with greater severity observed in DLB than in AD.

LPC and LPE are the products of phospholipase A2 (PLA2) hydrolyzing phosphatidylcholine (PC) and phosphatidylethanolamine (PE). They are significantly elevated in the plasma of DLB, suggesting possible enhanced PLA2 activity.[48] LPC/LPE have strong pro-inflammatory and pro-apoptotic properties. LPC and LPE exhibit potent pro-inflammatory and pro-apoptotic properties. Research demonstrates that LPC triggers endothelial cell apoptosis, including in brain microvascular endothelial cells (BMECs), compromises blood-brain barrier integrity, and increases vascular permeability.[49] LPC/LPE promote the release of inflammatory factors, monocyte infiltration, and glial cell activation by activating G protein-coupled receptors such as GPR4, exacerbating neuroinflammation.[50] DLB is frequently associated with earlier and more pronounced autonomic dysfunction and vascular impairment, such as orthostatic hypotension, and the vascular toxicity of LPC/LPE—characterized by endothelial apoptosis and impaired vasodilation—may be exacerbated in this context. Furthermore, LPC/LPE serve as essential intermediates in phospholipid remodeling of Lands cycle, and their accumulation may indicate accelerated membrane phospholipid turnover, potentially as a compensatory response to cellular stress, membrane injury, or inflammatory conditions.[51]

PA serves as a central intermediate in the biosynthesis of all glycerophospholipids and triacylglycerols and functions as a critical signaling lipid.[52] Elevated PA may result from the activation of phospholipase D (PLD), which hydrolyzes PC to produce PA. PA participates in the regulation of various processes, including activation of the AKT signaling pathway, cell proliferation, vesicle transport, and inflammatory responses.[53] Elevated PA may further amplify the neuroinflammation induced by LPC/LPE through promoting inflammatory signaling pathways. Therefore, the significant elevation of LPC/LPE and PA represents one of the most prominent features of the lipid profile in DLB plasma. They jointly point to possible enhanced phospholipase activity (PLA2, PLD), dysregulation of phospholipid remodeling, and intense neuroinflammatory state. These alterations may serve as both pathogenic drivers and potential biomarkers in DLB, specifically linked to processes such as α-synuclein aggregation and microglial activation, thereby distinguishing DLB from AD.

Furthermore, this study integrates five machine learning algorithms to systematically screen out the key lipid biomarkers for differential diagnosis of DLB and AD. Among them, PA (16:0_16:0) and PA (16:0_20:4) were identified by all algorithms, confirming their central role in disease classification. The diagnostic tool based on the lipid network should balance biological significance. LASSO regression method exhibits the best generalization ability in the test set and validation set, and its performance is significantly superior to models prone to overfitting such as SVM. The establishment of this model provides a reliable tool for effectively differentiating DLB from AD through non-invasive, easy-to-operate, and cost-effective plasma lipid metabolite levels.

The main advantages of this study are as follows: Firstly, based on the previous research of our team, for the first time, targeted lipidomics detection was conducted on patients with DLB and AD to determine the specific metabolic characteristics that can distinguish these two neurodegenerative diseases; Secondly, through multiple machine learning methods, a group of optimal differential metabolites were selected as biomarkers, which can effectively distinguish AD and DLB. The limitations of this study are as follows: First, no a priori power calculation was performed to determine the required sample size. Its single-center design and modest sample size precluded meaningful subgroup analyses (eg., by age or sex) to assess potential effect modification. Second, data on history of dyslipidemia and use of lipid-lowering medications were not systematically collected. As these factors may directly influence plasma lipid profiles, their absence represents a potential source of residual confounding. Future prospective studies should incorporate detailed metabolic and medication history to accurately characterize lipid metabolic differences between DLB and AD. Then, common bottlenecks in lipidomic biomarker studies include inter-laboratory variability, insufficient data standardization, and lack

of independent validation cohorts.[54] Although we implemented rigorous quality control measures—including pooled QC samples, CV-based filtering, and LOESS normalization—to minimize technical variation, these inherent limitations should be considered when interpreting our findings. Future multi-center studies with larger, more diverse populations are warranted to validate and refine the proposed lipid panel. The selected differential metabolites need to be further validated through animal experiments to clarify their causal relationship in the occurrence and development of the disease, and to deeply elucidate the specific mechanism of specific lipid molecules in DLB-related pathologies such as α-synuclein aggregation and neuroinflammation. Due to the lack of neuropathological confirmation as the gold standard, we were unable to provide definitive molecular pathological staging for patients and therefore could not perform stratification based on disease duration. Given that late-stage DLB patients frequently harbor co-existing AD pathology, the diagnostic efficacy of our method in this population may be confounded by mixed pathology.[1] Future validation in independent cohorts with detailed clinicopathological characterization and longitudinal follow-up is warranted to assess the stage-specific performance of our method.

Conclusion

This study, by integrating plasma lipidomics with machine learning algorithms, systematically revealed the metabolic differences between DLB and AD. Compared with AD patients, DLB patients exhibited characteristic lipid profiles with significantly elevated sphingolipids (Cer, SM), and substantial upregulation of lysophospholipids (LPC/LPE) and PA, etc. This study not only provides a new biomarker panel for the differentiation of DLB and AD, but also reconstructs the understanding of the pathological mechanism of DLB from a metabolic perspective, laying a foundation for the development of diagnostic strategies and therapeutic interventions targeting metabolic pathways. Nevertheless, external validation, workflow standardization, and mechanistic studies are required before clinical translation. Future research should prioritize longitudinal validation and integration with complementary biomarkers to enhance diagnostic precision and disease monitoring.

Data Sharing Statement

Data are available from the corresponding author upon reasonable request.

Ethics Approval and Consent to Participate

All procedures involving human participants in this study were approved by Ethics Committee of Xuanwu Hospital (No. [2020]097) and was conducted in accordance with the Declaration of Helsinki. Informed consent was obtained from all enrolled participants or their family members.

Consent for Publication

Not applicable. All data presented in this manuscript were rigorously reviewed and thoroughly anonymized. Any direct or indirect personal identifiers have been removed to protect participant privacy, ensuring that no individuals are identifiable.

Author Contributions

All authors made a significant contribution to the work reported, whether that is in the conception, study design, execution, acquisition of data, analysis and interpretation, or in all these areas; took part in drafting, revising or critically reviewing the article; gave final approval of the version to be published; have agreed on the journal to which the article has been submitted; and agree to be accountable for all aspects of the work.

Funding

This work were supported by National Key R&D Program of China (2024YFC2510204), Medical Science Research Project of Hebei20251630 and Postdoctoral Research Activity Funding Project of Beijing City.

Disclosure

There are no conflicts of interest.

References

1. Neupane S, Hortobágyi T. Molecular crossroads: shared and divergent molecular signatures in Alzheimer's disease and Dementia with Lewy bodies. *Int J Mol Sci*. 2025;26(24):11811. doi:10.3390/ijms262411811
2. Better MA. 2023 Alzheimer's disease facts and figures. *Alzheimers Dement*. 2023;19(4):1598–1695. doi:10.1002/alz.13016
3. Vann Jones SA, O'Brien JT. The prevalence and incidence of dementia with Lewy bodies: a systematic review of population and clinical studies. *Psychol Med*. 2014;44(4):673–683. doi:10.1017/s0033291713000494
4. Armstrong MJ, Alliance S, Corsentino P, DeKosky ST, Taylor A. Cause of death and end-of-life experiences in individuals with Dementia with Lewy bodies. *J Am Geriatr Soc*. 2019;67(1):67–73. doi:10.1111/jgs.15608
5. Wyman-Chick KA, Chrenka EAB, Kane JPM, et al. Utilization patterns and clinical factors associated with hospitalization in early-stage dementia with Lewy bodies. *Int J Geriatr Psychiatry*. 2025;40(7):e70125. doi:10.1002/gps.70125
6. McKeith IG, Boeve BF, Dickson DW, et al. Diagnosis and management of dementia with Lewy bodies: fourth consensus report of the DLB Consortium. *Neurology*. 2017;89(1):88–100. doi:10.1212/wnl.0000000000004058
7. Lau VZ, Awogbindin IO, Frenkel D, Whitehead SN, Tremblay M. A hypothesis explaining Alzheimer's disease, Parkinson's disease, and dementia with Lewy bodies overlap. *Alzheimers Dement*. 2025;21(6):e70363. doi:10.1002/alz.70363
8. Gezegen H, Alaylıoğlu M, Şahin E, et al. Unravelling the plasma proteome: pioneering biomarkers for differential dementia diagnosis. *Alzheimers Dement*. 2025;21(7):e70162. doi:10.1002/alz.70162
9. Choudhury P, Zhang N, Adler CH, et al. Longitudinal motor decline in dementia with Lewy bodies, Parkinson disease dementia, and Alzheimer's dementia in a community autopsy cohort. *Alzheimers Dement*. 2023;19(10):4377–4387. doi:10.1002/alz.13357
10. Bonomi CG, Martorana A, Motta C, et al. Autonomic dysfunction in patients with dementia with Lewy bodies and its relationship with nigrostriatal denervation. *Neurology*. 2025;104(8):e213463. doi:10.1212/wnl.0000000000213463
11. Palmqvist S, Whitson HE, Allen LA, et al. Alzheimer's Association Clinical Practice Guideline on the use of blood-based biomarkers in the diagnostic workup of suspected Alzheimer's disease within specialized care settings. *Alzheimers Dement*. 2025;21(7):e70535. doi:10.1002/alz.70535
12. Vanherle S, Loix M, Miron VE, Hendriks JJA, Bogie JFJ. Lipid metabolism, remodelling and intercellular transfer in the CNS. *Nat Rev Neurosci*. 2025;26(4):214–231. doi:10.1038/s41583-025-00908-3
13. Johnson DH, Kou OH, White JM, et al. Lipid packing defects are necessary and sufficient for membrane binding of α-synuclein. *Commun Biol*. 2025;8(1):1179. doi:10.1038/s42003-025-08622-7
14. Area-Gómez E, Fanning S, Dettmer U. Lipid alterations and pathogenic roles in synucleinopathies. *Cold Spring Harb Perspect Med*. 2025. doi:10.1101/cshperspect.a041646
15. Erskine D, Bronowska AK, Outeiro TF, Attems J. Sphingolipidoses: expanding the spectrum of α-synucleinopathies. *J Neural Transm*. 2025. doi:10.1007/s00702-025-02925-z
16. Gregorio I, Russo L, Torretta E, et al. GBA1 inactivation in oligodendrocytes affects myelination and induces neurodegenerative hallmarks and lipid dyshomeostasis in mice. *Mol Neurodegener*. 2024;19(1):22. doi:10.1186/s13024-024-00713-z
17. Avenali M, Blandini F, Cerri S. Glucocerebrosidase defects as a major risk factor for Parkinson's disease. *Front Aging Neurosci*. 2020;12:97. doi:10.3389/fnagi.2020.00097
18. Shen H, Yu Y, Wang J, Nie Y, Tang Y, Qu M. Plasma lipidomic signatures of dementia with Lewy bodies revealed by machine learning, and compared to Alzheimer's disease. *Alzheimers Res Ther*. 2024;16(1):226. doi:10.1186/s13195-024-01585-7
19. Salek RM, Steinbeck C, Viant MR, Goodacre R, Dunn WB. The role of reporting standards for metabolite annotation and identification in metabolomic studies. *Gigascience*. 2013;2(1):13. doi:10.1186/2047-217x-2-13
20. Ruiz-Canela M, Hruby A, Clish CB, Liang L, Martínez-González MA, Hu FB. Comprehensive metabolomic profiling and incident cardiovascular disease: a systematic review. *J Am Heart Assoc*. 2017;6(10). doi:10.1161/jaha.117.005705
21. Wei R, Li G, Seymour AB. High-throughput and multiplexed LC/MS/MRM method for targeted metabolomics. *Anal Chem*. 2010;82(13):5527–5533. doi:10.1021/ac100331b
22. Jack CR Jr, Bennett DA, Blennow K, et al. NIA-AA research framework: toward a biological definition of Alzheimer's disease. *Alzheimers Dement*. 2018;14(4):535–562. doi:10.1016/j.jalz.2018.02.018
23. Mueller C, Ballard C, Corbett A, Aarsland D. The prognosis of dementia with Lewy bodies. *Lancet Neurol*. 2017;16(5):390–398. doi:10.1016/s1474-4422(17)30074-1
24. Chiu SY, Chen R, Wang WE, et al. Longitudinal free-water changes in dementia with Lewy bodies. *Mov Disord*. 2024;39(5):836–846. doi:10.1002/mds.29763
25. Yu Y, Wang J, Li D, Lu Y, Lu L, Qu M. Application of mini-mental state examination and Montreal Cognitive Assessment in the diagnosis of dementia with Lewy bodies and Alzheimer's disease. *Appl Neuropsychol Adult*. 2025;1–10. doi:10.1080/23279095.2025.2478204
26. Frölich N, Klose C, Widén E, Ripatti S, Gerl MJ. Imputation of missing values in lipidomic datasets. *Proteomics*. 2024;24(15):e2300606. doi:10.1002/pmic.202300606
27. Linn KA, Gaonkar B, Doshi J, Davatzikos C, Shinohara RT. Addressing confounding in predictive models with an application to neuroimaging. *Int J Biostat*. 2016;12(1):31–44. doi:10.1515/ijb-2015-0030
28. Zhang D, Zhang M. Advanced statistical methods for NMR-based metabolomics. *Methods Mol Biol*. 2019;2037:471–482. doi:10.1007/978-1-4939-9690-2_26
29. Ou M, Song Y, Li S, et al. LC-MS/MS method for serum creatinine: comparison with enzymatic method and Jaffe method. *PLoS One*. 2015;10(7):e0133912. doi:10.1371/journal.pone.0133912
30. Raben DM, Barber CN. Phosphatidic acid and neurotransmission. *Adv Biol Regul*. 2017;63:15–21. doi:10.1016/j.jbior.2016.09.004

31. Dahabiyeh LA, Nimer RM, Rashed M, Wells JD, Fiehn O. Serum-based lipid panels for diagnosis of idiopathic Parkinson's disease. *Metabolites*. 2023;13(9):990. doi:10.3390/metabo13090990
32. Thakkar H, Vincent V, Chaurasia B. Ceramide signaling in immunity: a molecular perspective. *Lipids Health Dis*. 2025;24(1):225. doi:10.1186/s12944-025-02642-2
33. Shen X, Feng R, Zhou R, Zhang Z, Liu K, Wang S. Ceramide as a promising tool for diagnosis and treatment of clinical diseases: a review of recent advances. *Metabolites*. 2025;15(3):195. doi:10.3390/metabo15030195
34. Li H, Xiao Q, Zhu L, Kang J, Zhan Q, Peng W. Targeting ceramide-induced microglial pyroptosis: icariin is a promising therapy for Alzheimer's disease. *J Pharm Anal*. 2025;15(4):101106. doi:10.1016/j.jpha.2024.101106
35. Kalkman HO, Smigielski L. Ceramides may play a central role in the pathogenesis of Alzheimer's disease: a review of evidence and horizons for discovery. *Mol Neurobiol*. 2025;62(11):14424–14441. doi:10.1007/s12035-025-04989-0
36. Xiao S, Wei X, Han B, et al. Quantitative analysis of targeted lipidomics in the hippocampus of APP/PS1 mice employing the UHPLC-MS/MS method. *Front Aging Neurosci*. 2025;17:1561831. doi:10.3389/fnagi.2025.1561831
37. Gao X, Cheng X, Chen P, et al. Plasma lipidomic fingerprinting enables high-accuracy biomarker discovery for Alzheimer's disease: a targeted LC-MRM/MS approach. *Geroscience*. 2025. doi:10.1007/s11357-025-01777-5
38. Chua XY, Torta F, Chong JR, et al. Lipidomics profiling reveals distinct patterns of plasma sphingolipid alterations in Alzheimer's disease and vascular dementia. *Alzheimers Res Ther*. 2023;15(1):214. doi:10.1186/s13195-023-01359-7
39. Choudhary P, Kumari S, Bagri K, Deshmukh R. Ceramide: a central regulator in Alzheimer's disease pathogenesis. *Inflammopharmacology*. 2025;33(4):1775–1783. doi:10.1007/s10787-025-01719-9
40. Usenko TS, Senkevich KA, Bezrukova AI, et al. Impaired sphingolipid hydrolase activities in dementia with Lewy bodies and multiple system atrophy. *Mol Neurobiol*. 2022;59(4):2277–2287. doi:10.1007/s12035-021-02688-0
41. Taniguchi M, Okazaki T. Role of ceramide/sphingomyelin (SM) balance regulated through "SM cycle" in cancer. *Cell Signal*. 2021;87:110119. doi:10.1016/j.cellsig.2021.110119
42. Xiang H, Jin S, Tan F, Xu Y, Lu Y, Wu T. Physiological functions and therapeutic applications of neutral sphingomyelinase and acid sphingomyelinase. *Biomed Pharmacother*. 2021;139:111610. doi:10.1016/j.biopha.2021.111610
43. Kim WS, Halliday GM. Changes in sphingomyelin level affect alpha-synuclein and ABCA5 expression. *J Parkinsons Dis*. 2012;2(1):41–46. doi:10.3233/jpd-2012-11059
44. Llano DA, Devanarayan V. Serum phosphatidylethanolamine and lysophosphatidylethanolamine levels differentiate Alzheimer's disease from controls and predict progression from mild cognitive impairment. *J Alzheimers Dis*. 2021;80(1):311–319. doi:10.3233/jad-201420
45. Kurano M, Saito Y, Uranbileg B, et al. Modulations of bioactive lipids and their receptors in postmortem Alzheimer's disease brains. *Front Aging Neurosci*. 2022;14:1066578. doi:10.3389/fnagi.2022.1066578
46. Michno W, Bowman A, Jha D, et al. Spatial neurolipidomics at the single amyloid-β plaque level in postmortem human Alzheimer's disease brain. *ACS Chem Neurosci*. 2024;15(4):877–888. doi:10.1021/acschemneuro.4c00006
47. Pan X, Donaghy PC, Roberts G, et al. Plasma metabolites distinguish dementia with Lewy bodies from Alzheimer's disease: a cross-sectional metabolomic analysis. *Front Aging Neurosci*. 2023;15:1326780. doi:10.3389/fnagi.2023.1326780
48. Wuhanqimuge, Itakura A, Matsuki Y, Tanaka M, Arioka M. Lysophosphatidylcholine enhances NGF-induced MAPK and Akt signals through the extracellular domain of TrkA in PC12 cells. *FEBS Open Bio*. 2013;3(1):243–251. doi:10.1016/j.fob.2013.05.003
49. Yan S, Chai H, Wang H, et al. Effects of lysophosphatidylcholine on monolayer cell permeability of human coronary artery endothelial cells. *Surgery*. 2005;138(3):464–473. doi:10.1016/j.surg.2005.06.027
50. Liu T, Wang X, Guo F, et al. Lysophosphatidylcholine induces apoptosis and inflammatory damage in brain microvascular endothelial cells via GPR4-mediated NLRP3 inflammasome activation. *Toxicol In Vitro*. 2021;77:105227. doi:10.1016/j.tiv.2021.105227
51. Law SH, Chan ML, Marathe GK, Parveen F, Chen CH, Ke LY. An Updated Review of Lysophosphatidylcholine Metabolism in Human Diseases. *Int J Mol Sci*. 2019;20(5). doi:10.3390/ijms20051149
52. Bermúdez V, Tenconi PE, Giusto NM, Mateos MV. Canonical phospholipase D isoforms in visual function and ocular response to stress. *Exp Eye Res*. 2022;217:108976. doi:10.1016/j.exer.2022.108976
53. Tanguy E, Wang Q, Moine H, Vitale N. Phosphatidic Acid: from Pleiotropic Functions to Neuronal Pathology. *Front Cell Neurosci*. 2019;13:2. doi:10.3389/fncel.2019.00002
54. Malarvannan M, Naik Sabavath BT, Soni N, Mihir Mandar C, Paul D. Exploring lipidomics in biomarker discovery. *Clin Chim Acta*. 2026;579:120698. doi:10.1016/j.cca.2025.120698